

Synergetic enhanced day-light driven photocatalytic reduction of heavy metal Cr(VI) by graphene supported ZnO nanocubes

P. V. Ramana¹, A. Viswadevarayulu¹, K. Kumar², S. Adinarayana Reddy^{1*}

¹Department of Materials Science & Nanotechnology, Yogi Vemana University, Kadapa 516003, Andhra Pradesh, India

²Central analytical lab, BITS-Pilani-Hyderabad campus, Hyderabad 500078, Telangana, India

*Corresponding author. Tel: (+91) 9491310368; E-mail: anreddyphd@gmail.com

Received: 03 September 2016, Revised: 19 October 2016 and Accepted: 06 November 2016

DOI: 10.5185/amlett.2017.7057

www.vbripress.com/aml

Abstract

The potential of a novel photocatalyst graphene-ZnO (G-ZnO) obtained from graphene oxide and zinc acetate dihydrate was investigated for the reduction of heavy metal Cr(VI) ions from water. In which ZnO nanocubic crystals were finely doped on the graphene sheets, was well done by facile wet chemical/reflux method under N₂ atmosphere. Due to hindered nature of photo-generated electron-hole pair recombination and enhanced light absorption shows efficient photocatalytic performance of G-ZnO nanocomposites (NCs) in the reduction of Cr(VI) ions with a degradation rate of 98% under daylight illumination as related with bare ZnO (42%), graphene oxide (GO) (19%) and mechanical mixture GO+ZnO (62%). The overall results demonstrated that the photocatalyst used in this study, is promising, efficient and economical when used to separate heavy metal ions from water. Copyright © 2017 VBRI Press.

Keywords: ZnO cubes, graphene sheet, photocatalyst, day-light, nanocomposite.

Introduction

Water purification/technology, photocatalysis is a promising approach for the elimination of unfavorable organic compounds, waste water treatment of inorganic pollutants and can also be applied to the removal of air pollutants in an enclosed environment [1]. The heavy metals are well known water pollutants, which are highly toxic, non-ecofriendly and resistant to direct degradation or reduction by day-light driven and are consequently classified as importunate pollutants [2]. The release and subsequent accumulation of these toxic compounds in aquatic media create extreme risk to the environment. Chromium (Cr) species are produced by different industrial routes like dyeing, printing, tanning and electroplating. Even though both chromium species are toxic in nature. Environmentally stable oxidation state of Cr(III) is harmless, non-toxic in nature, not having mobility property and also easily isolated from water as compared with Cr(VI) ion [3, 4]. For the reason that, lots of scientists have concentrated on Cr(VI) removal from water. The most current, efficient and economical method to remove heavy metals by photocatalytic degradation using day-light driven in the presence of an appropriate photocatalyst that is able to promote the reduction of toxic metals to favorable byproducts.

Graphene has high chemical stability and versatile platform for photocatalysis due to specific surface area (2630 m²/g), excellent electrical conductivity and outstanding optical transmittance [5]. At present major

problems affecting the mankind are energy crisis and environmental problems. The potential solution of these problems is utilization of solar energy for photocatalytic degradation using suitable semiconducting photocatalysts. In the process of photocatalysis, graphene to enhancing the separation and exchange of photo-generated charge carriers from semiconductors [6, 7]. Many researchers have synthesized a number of graphene-supported semiconductors such as graphene-ZnO, graphene-CdS/ZnO, graphene-TiO₂, RGO- α -Fe₂O₃ nanorod and Au/graphene nanocomposite for the removal of water pollutants as organic and inorganic to enhance its catalytic activity [8-14]. On the other hand, reusability of catalysts for further use is crucial problem. Therefore, researchers have tried to improve distinguishable nanocomposite/nanoparticles for reduction of heavy metal ions to overcome this tricky. Hybridization of graphitic materials with ZnO offers the efficient photocatalytic activity [15, 16]. Compared some other semiconductor oxides, ZnO with the band gap of 3.3 eV, is being widely used as an effective and non-toxic photocatalyst. ZnO, which is inexpensive and stable under ambient conditions, may be an ideal compound for use in clean technology. Additionally, due to its outstanding characteristics and suitable band gap, ZnO is identified as one of the best photocatalytic materials [17, 18].

But to the best of our knowledge, only a few reports exist on unmodified and co-catalyst-free graphene-ZnO nanostructures for Cr(VI) reduction. For example, Liu et

al., demonstrated the photocatalytic reduction of Cr(VI) using ZnO-graphene photocatalyst under UV light illumination [19, 20]. In addition to that nanostructured materials are promising for effective utilization of solar energy for photocatalytic degradation due to their nanostructured properties, high quantum yield, efficient electron-hole properties, etc. Wang et al., explored the high photocatalytic degradation of dyes and Cr(VI) by Graphene-CNTs-TiO₂ composites under UV-light irradiation [21]. The present study exploits the preparation of photocatalyst graphene-ZnO (G-ZnO) by wet chemical/reflux method for synergetic enhanced of photocatalytic reduction of Cr(VI) from water under daylight driven as related with GO, ZnO, mechanical mixture GO+ZnO and also calculated re-usability of photocatalyst.

Experimental

Synthesis of graphite oxide

Modified Hummers method was suitable procedure for synthesis of graphite oxide from graphite [22], about 5g of graphite was mixed to 115 mL of concentrated H₂SO₄ (98%) in an ice bath with magnetically stirring for 30 min. A 15 g of KMnO₄ was mixed little by little to the above dispersion with constant magnetic stirring and cooling for 30 min. Then, 2.5 g of NaNO₃ was added with nonstop magnetic stirring at 30 °C for 1 hour. Below 15 °C temperature should be maintained at the time of mixing. The temperature of the reaction mixture then increased to 40 °C with water bath and magnetic stirring of this suspension should be done constantly for 30 min. Then, the mixture was diluted by approx. one liter of

increased to 98 °C. Hydrogen peroxide (30%) was mixed to the reaction mixture and the mixture turned from black to yellow colour. Until the arrival of reaction mixture at pH=7 and it was washed under centrifugation for several times with 1M HCl (5%) and again with double distilled water. Graphite oxide was obtained by drying the product in vacuum oven at 60 °C for overnight.

Synthesis of graphene-ZnO NCs

The graphene-ZnO (G-ZnO) NCs were produced by wet chemical method [23]; the graphite oxide was dissolved in ethanol (0.002 g/L) and water bath sonicated to get graphene oxide suspension for 1 h. The suspension was stable for several months with no precipitation and then zinc acetate dihydrate (0.880 g) was dissolved in 0.40 L of ethanol was added under magnetic stirring for the production of G-ZnO mixture. NaOH solution was added to the reaction mixture and its pH value was move to 9.0. It should be stirred continuously up to 30 min. Afterwards, the reaction of mixture was allowed at 140 °C under N₂ atmosphere for 24 h. Ethanol was used to the prepared composites on first on first basis, it is washed and centrifuged. Double distilled water was added to it and washed it for several times and then this final material was dried at 60 °C for overnight. The synthetic procedure was shown in (Fig. 1).

Photocatalytic activity studies

Photocatalytic experiments were conducted under daylight driven in sunny days between 11.30 AM and 2.30 PM. In this typical process, prepared 0.03 g of photocatalyst was added to 0.30 L Cr(VI) aqueous

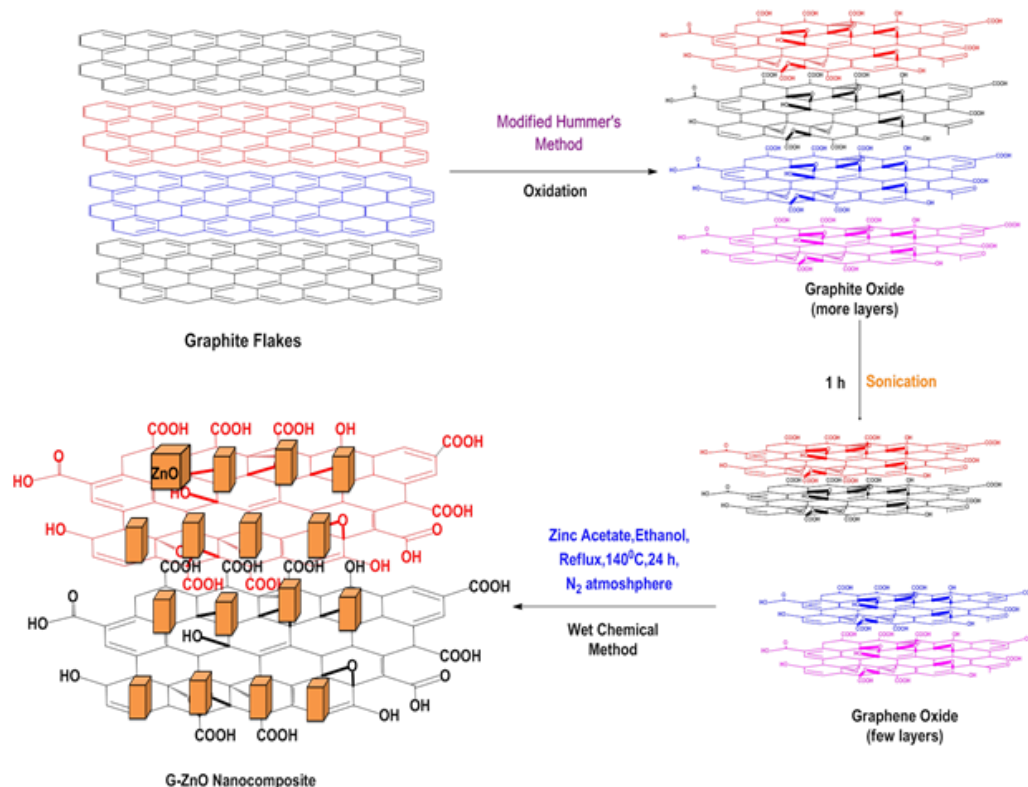


Fig.1. Scheme illustration of the preparation procedure of G-ZnO nanocomposite.

double distilled water, the temperature of which then

solution with a concentration of 0.014 g/L in a glass

beaker. To attain excellent equilibrium of absorption and desorption between G-ZnO and heavy metal ions Cr(VI) by placing in ultra-sonic water bath for 5 min and then stirred at room temperature for 1h. 3 mL of the suspension was taken to the equilibrium position to find first concentration of Cr(VI) solution, which was denoted as base concentration C_0 . Subsequently this mixed suspension is exposed to day-light, which light intensity was approximately one lakh lux, calculated by TESLA lux meter, for 60 min and 3 mL of the sample has to be taken in sample vials for every 10, 20, 30, 40, 50 and 60 min. After exposing to day-light, immediately isolated to any suspended material by centrifugation method. The UV-visible spectrum of the supernatant was noted by UV-visible spectrometer to calculate the concentration of heavy metal Cr(VI) at optical absorption at 365 nm, which designated as C_t . The absorbance at maximum wavelength (λ_{max}) of Cr(VI) pollutant (372 nm) was determined by UV-Vis spectrophotometer.

Results and Discussion

XRD is a very important experimental technique has been used to determine the crystal structure of; solids, including lattice constants and geometry, identification of unknown materials, orientation of single crystals, preferred orientation of poly-crystals, defects, stresses, etc. The unknown crystal structure of the materials can be identified by matching with standard diffraction pattern of the similar with JCPDS data as reference. From (Fig. 2 left a) exhibits sharp crystalline peaks at 26.46° and 9.92° which represents the graphite and graphite oxide respectively. Finally, analyzed ZnO crystalline peaks consisted with G-ZnO composite was found at $31.73, 34.37, 36.21, 47.48, 56.53, 62.77, 66.30, 67.86, 69.00, 72.46,$ and 76.86° are indicated to (100), (002), (101), (102), (110), (103), (200), (112), (201), (004) and (202) respectively (JCPDS number 89-1397). The broader peak at 13° was noticed in the nanohybrid material (G-ZnO), which is equivalent to the diffraction patterns of graphene [24].

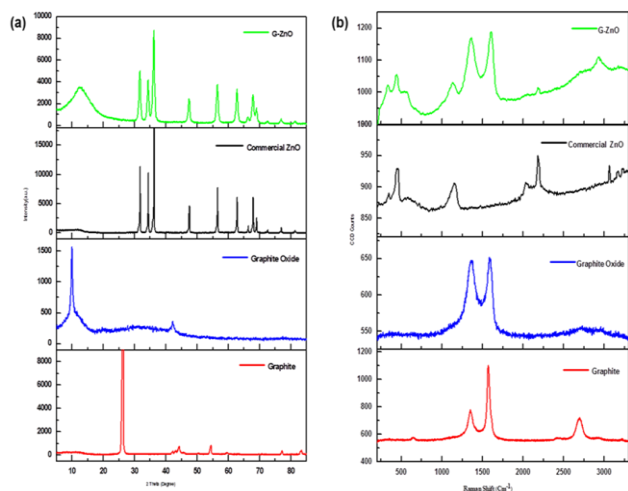


Fig.2. (Left) Typical P-XRD patterns of (a) G-ZnO (b) Commercial ZnO (c) Graphite Oxide and (d) Graphite and (right) Raman spectra of (a) G-ZnO composite (b) Commercial ZnO (c) Graphite Oxide and (d) Graphite photocatalysts.

The presence of both graphitic carbon and ZnO NPs can be deep-rooted from the Raman spectroscopy. From (Fig. 2 right b) clearly expressed the D and G bands at 1361 cm^{-1} and 1607 cm^{-1} , which corresponds to graphene. Peaks at $342, 452, 583$ and 1149 cm^{-1} were assigned to the ZnO [25]. The intensity of these peaks was reduced in NCs as similar to that in ZnO due to the intercalations of the ZnO and graphene sheets.

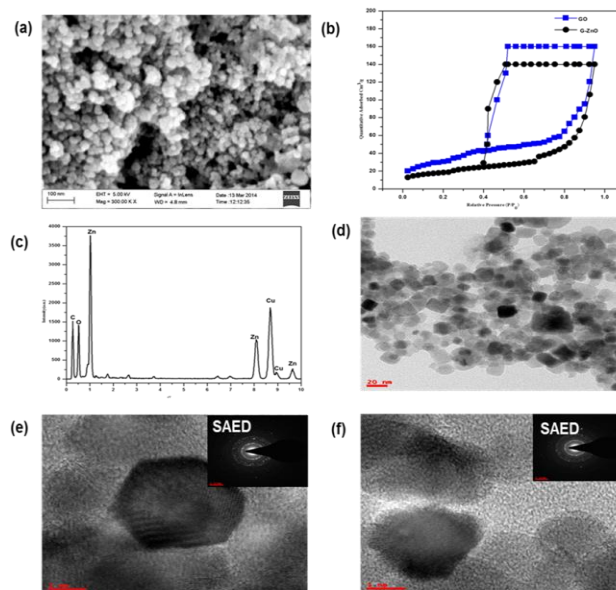


Fig.3. (a) FESEM images (b) N_2 adsorption-desorption, (c) EDAX studies (d) TEM (e and f) HRTEM images (inside SAED pattern of corresponding Graphene and ZnO) of G-ZnO nanocomposite.

The surface morphology of the synthesized G-ZnO NCs was measured by FESEM images as shown in (Fig. 3a). From the SEM images it is unambiguous that the morphology of intercalated NCs particles are really in nano size and it shows the graceless morphology due to the aggregation of particles in the solution while synthesis. If one can observe in depth we found that some of the places there is voids are observed, which are the responsible for the adsorption of Cr(VI) as well as photocatalytic performance of the final product. One can logically argue that these voids definitely because of the layered structure of graphene some of the voids are blocked because of anchoring of metal oxide nanoparticles into the free voids due to inhomogeneous distribution of metal oxide nanoparticles we can see some of the free voids in the SEM images.

N_2 adsorption-desorption isotherms of GO and G-ZnO NCs were shown in (Fig. 3b). It reveals that synthesized photocatalyst having both adsorption and desorption property. In general, the surface area of the catalyst is the most important factor in influencing the catalytic activity. Surface area of G-ZnO ($158.0\text{ m}^2\text{ g}^{-1}$) was lower than that of GO ($186.5\text{ m}^2\text{ g}^{-1}$) due to the high density and low surface area of ZnO cubes, which is beneficial towards enhancing photocatalytic activity. Zn, O, C and Cu elements were appeared in EDAX spectrum for concluding the G-ZnO composite as shown in (Fig. 3c). Cu element was looked in EDAX spectrum due to copper mesh substrate was used in HRTEM.

TEM images of the sample were recorded by pre-sonicating the sample in ethanol for 3 h for well distribution of particles, then after one drop of the sample drop casted on carbon coated TEM copper Grids 200 mesh at 200 kV. From the TEM images (**Fig. 3d**) it is lucid that there are two types of morphological observations found, one is accounted for graphene another one is ZnO nanoparticles. Graphene in the hexagonal arrangement whereas ZnO in cubic morphology. Both are in a luminous type and are in nanometer range around the 10-15 nm size.

In HRTEM we observed springes on the both layers when focused on them individually, where as in case of graphene which is in hexagonal arrangement shows this, whereas ZnO also shows springes which are in cubic form as shown in (**Fig. 3e**). HRTEM images of ZnO clearly identified the cubic arrangement as shown in (**Fig. 3f**) and also graphene observed the hexagonal arrangement. Moreover, their good crystallinity was verified by the SAED pattern as shown in (**Fig. 3 inside e and f**). The density of ZnO nanocubes on graphene is higher, which is very essential for photocatalytic activity of catalyst.

X-ray photoelectron spectroscopy (XPS) was utilized to analyze the surface chemical composition of the pristine and nanocomposite materials. Fortuitous carbon at a binding energy of 284.6 eV was used to get data through calibration. Except Zn, O and C, none elements were observed by composite of XPS analysis spectrum was shown in (**Fig. 4a**). Peaks at 1022.7 and 1045.7 eV indicated the Zn 2p_{3/2} and Zn 2p_{1/2} orbitals respectively were shown in (**Fig. 4b**). Two dissimilar kinds of peaks showed by oxygen species at 530.9 and 532.3 eV, which represents the ZnO lattice of oxygen and surface chemisorbed oxygen respectively, were shown in (**Fig. 4c**). C 1s exhibited three peaks at 285.0, 286.2 and 289.1 eV due to C-C (Sp²), C=O and C=C of graphene respectively were shown in (**Fig. 4d**) [26].

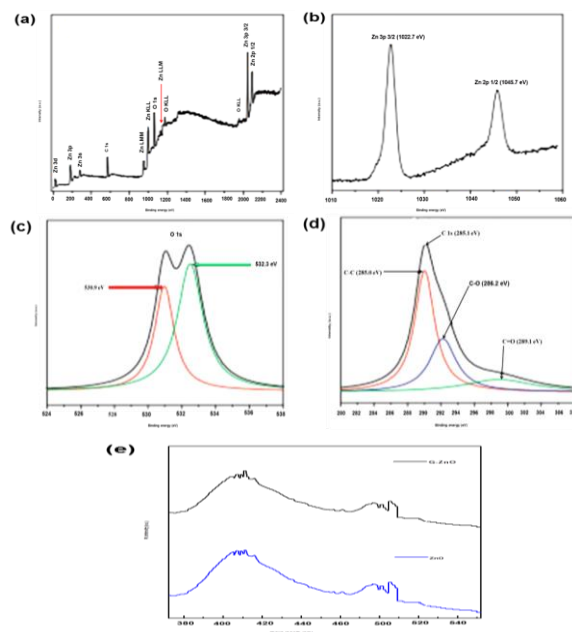


Fig. 4. (a) XPS analysis spectra (b) high resolution spectra of Zn 2p region (c) O 1s region (d) C 1s region for G-ZnO nanocomposite and (e) PL spectra of ZnO and G-ZnO with excitation wavelength of 325 nm.

The photoluminescence (PL) emission spectra can be used to investigate the fate of photo-generated electrons and holes in a semiconductor, since PL emission results from the recombination of free carriers. PL emission spectrum is useful to disclose the efficiency of charge carrier trapping, immigration, and transfer. In (**Fig. 4e**) shows the G-ZnO peak intensity lower the ZnO peak due to graphene to enhancing the separation and exchange of photogenerated charge carriers from semiconductors.

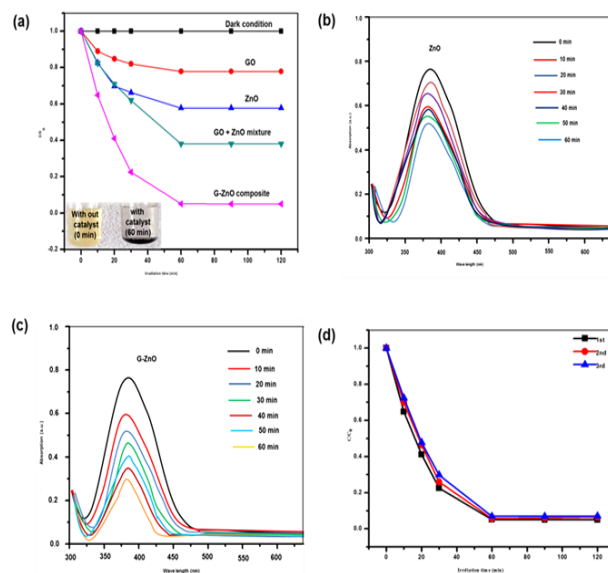


Fig. 5. (a) Comparison studies of dark, GO, ZnO, mechanical mixture GO+ZnO and G-ZnO at 14 mgL⁻¹ concentration of Cr(VI) solution (b) (c) UV-Vis absorbance spectrums of photocatalytic reduction of Cr(VI) (d) re-stability of G-ZnO by investigating its photocatalytic activity under solar light irradiation with three times of cycling uses.

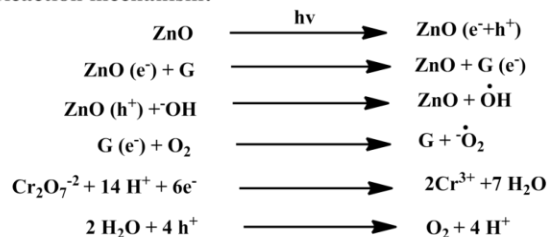
To illustrate the synergetic enhance of photocatalytic performance of G-ZnO NCs toward a heavy metal Cr(VI) ions, the daylight driven photocatalytic reduction of Cr(VI) in water was carried out at regular time intervals. The absorption of these solutions diminished steadily with illumination time. The typical absorption of heavy metal Cr(VI) nearly vanished and yellow colour of the Cr(VI) solution was transferred steadily to colourless for 1h. Photodegradation of Cr(VI) with G-ZnO NCs was shown in the (**Fig. 5a**). G-ZnO photocatalyst did not be degraded the Cr(VI) under the dark situation. At concentration 0.014 g/L of Cr(VI) degradation was 98%, which shows the G-ZnO NCs was an excellent photocatalyst. The degradation rate of Cr(VI) of ZnO was 42%, graphite oxide was 15% and mechanical mixing of GO+ZnO was 62%. The G-ZnO NCs has higher photocatalytic activity performance than others such as bare ZnO, GO and mechanical mixture of GO+ZnO. The typical absorption intensity of peak for the potassium dichromate diminished slowly with increasing time due to reduction of Cr(VI) ions as shown in (**Fig. 5 b and c**).

Recycling of the catalyst is the very crucial factor to decide the sustainability of the photocatalyst. After completion of the photocatalysis process, the recyclability test was estimate the skill of the catalyst and we found that the G-ZnO NCs shall be reused again and again to achieve reduction of Cr(VI). After degradation, separation of the photocatalyst was done by simple washed several

times with distilled water and dried in a hot air oven at 80 °C for 60 min. At that time, fresh Cr(VI) solution was mixed with the photocatalyst and degradation technique was explored under day-light driven. No significant change of photocatalytic activity of G-ZnO NCs was observed up to three cycles. Conversely, trivial loss of catalytic activity was found due to unavailability of the active surface site on the G-ZnO NCs surface in each cycle [27-29]. In the first cycle 98 % of Cr(VI) reduction efficiency was noticed. After three cycles, reduction efficiency extended up to 92% for Cr(VI) ions. So, G-ZnO nanocomposite shows tremendous reusability for reduction of these Cr(VI) ions as shown in the (Fig. 5d).

In general, a sensitized photocatalytic oxidation process is one in which a semiconductor upon absorption of a photon of suitable energy can act as a photocatalytic substrate by producing highly reactive radicals that can reduce inorganic compounds. By applying the daylight on NCs, ZnO surface formed electron-hole pairs and these generated photo electrons transferred into graphene sheet due to strongly contact on the surface of the ZnO cubes. Effective charge separation was kept up on NCs because graphene act as electron acceptor [30-36]. Dissolved oxygen species reacts with trapped electrons of graphene to produce reactive oxygen species, which leads to diminish the electron-hole recombination rate between the graphene and ZnO. Moreover, ZnO surface containing electrons also reacts with dissolved oxygen to get reactive oxygen species. Finally, produces hydroxyl ($\bullet\text{OH}$) free radicals due to reacts with water and reactive oxygen species. These hydroxyl free radicals were reacting with the contaminant present in the water and degraded as shown in (Fig. 6) [37-42]. In the photocatalytic reduction process, the electrons generated at the conduction band helps in the reduction of Cr(VI) to non-toxic Cr(III) [47-49]. The reaction mechanism was shown in below:

Reaction mechanism:



Conclusion

A simple and effective method was established to prepare G-ZnO photocatalyst by using graphene and ZnO. Excellent circulated ZnO nanocubes with an average size ranged between 10-15 nm were deposited on graphene via the wet chemical method. G-ZnO nanocomposite effectively reduces mutagenic aqueous solution of Cr(VI) to non-toxic aqueous solution of Cr(III) under natural daylight driven. The re-stability of the composite was analyzed. Graphene based composite materials indication good-looking environmental applications such as toxic pollutants removal in terms of their cheap cost, simple handling and high degradation performance. Hence, photocatalytic reduction using G-ZnO nanocomposite is a

most suitable, suitable and low cost effective technique for further treatment of industrial wastewater.

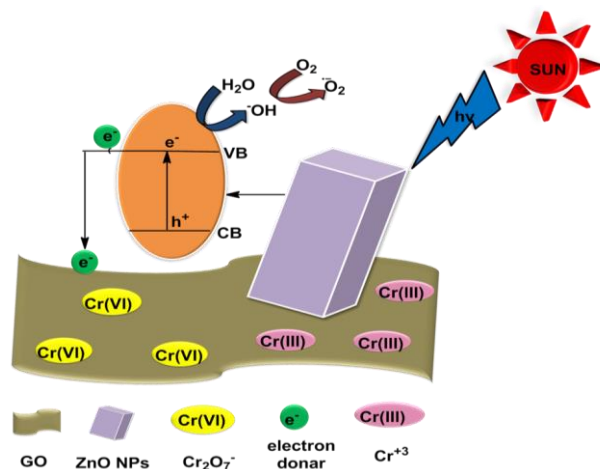


Fig. 6. Proposed reaction mechanism of Cr(VI) reduction by G-ZnO nanocomposite.

Acknowledgements

Funding in support of this work was provided by the University Grant Commission (UGC), New Delhi [Grant no.2-362/2013 (SR)]. Sri Venkateswara University, Tirupati, University of Hyderabad, Hyderabad, IIT Madras, Chennai and IICT Hyderabad are gratefully acknowledged for instrumental measurements. We are also thankful to Dr R V Jayanth Kasyap, Asst. Professor in English, Yogi Vemana University, Kadapa, India, for verifying the linguistic correctness.

References

- Andrew, M.; Richard, H. D.; David, W.; *Chem. Soc. Rev.*, **1993**, 22, 417.
DOI: [10.1039/CS9932200417](https://doi.org/10.1039/CS9932200417)
- Yu, S. H.; Li, H.; Yao, Q.; Fu, S. Q.; Zhou, G. T.; *RSC Adv.*, **2015**, 5, 84471.
DOI: [10.1039/C5RA14130C](https://doi.org/10.1039/C5RA14130C)
- Fang, T.; Yang, X.; Zhang, L.; Gong, J.; *J. Hazard. Mater.*, **2016**, 312, 106.
DOI: [10.1016/j.jhazmat.2016.03.046](https://doi.org/10.1016/j.jhazmat.2016.03.046)
- Dai, Y.; Hu, Y.; Jiang, B.; Zou, J.; Tian, G.; Fu, H.; *J. Hazard. Mater.*, **2016**, 309, 249.
DOI: [10.1016/j.jhazmat.2015.04.013](https://doi.org/10.1016/j.jhazmat.2015.04.013)
- Xiang, Q. J.; Yu, J. G.; Jaroniec, M.; *Chem. Soc. Rev.*, **2012**, 41, 782.
DOI: [10.1039/C1CS15172J](https://doi.org/10.1039/C1CS15172J)
- Ramana, P.V.; Viswadevarayalu, A.; Janardhan Reddy, K.; Prathima, B.; Madhavi, V.; Adinarayana Reddy, S.; *J. Expt. Nanosci.*, **2016**, 11, 722.
DOI: [10.1080/17458080.2016.1144937](https://doi.org/10.1080/17458080.2016.1144937)
- Zhang, N.; Yang M.Q.; Liu, S.; Sun, Y.; Xu Y. J.; *Chem. Rev.*, **2015**, 115, 10307.
DOI: [10.1021/acs.chemrev.5b00267](https://doi.org/10.1021/acs.chemrev.5b00267)
- Moussa, H.; Girot, E.; Mozet, K.; Alem, H.; Medjahdi, G.; Schneider, R.; *Appl. Cataly. B: Environ.*, **2016**, 185, 11.
DOI: [10.1016/j.apcatb.2015.12.007](https://doi.org/10.1016/j.apcatb.2015.12.007)
- Zhang, N.; Zhang, Y.; Xu, Y. J.; *Nanoscale*, **2012**, 4, 5792.
DOI: [10.1039/C2NR31480K](https://doi.org/10.1039/C2NR31480K)
- Wang, T.; Li, C.; Ji, J.; Wei, Y.; Zhang, P.; Wang, S.; Fan, X.; *ACS Sustainable Chem. Eng.*, **2014**, 2, 2253.
DOI: [10.1021/sc5004665](https://doi.org/10.1021/sc5004665)
- A. Tiwari, M. Syväjärvi (Eds), In *Advanced 2D Materials*, John Wiley & Sons, Beverly, MA, USA, **2016**.
- Xiong, Z.; Zhang, L. L.; Ma, J.; Zhao, X. S.; *Chem. Commun.*, **2010**, 46, 6099.
DOI: [10.1039/C0CC01259A](https://doi.org/10.1039/C0CC01259A)
- Han, W.; Ren, L.; Qi, X.; Liu, Y.; Wei, X.; Huang, Z.; Zhong, J.; *J. Appl. Surf. Sci.*, **2014**, 299, 12.

- DOI: [10.1016/j.apsusc.2014.01.170](https://doi.org/10.1016/j.apsusc.2014.01.170)
14. Li, B.; Cao, H.; *J. Mater. Chem.*, **2011**, *21*, 3346.
DOI: [10.1039/C0JM03253K](https://doi.org/10.1039/C0JM03253K)
 15. Yang, M. Q.; Xu, Y. J.; *J. Phys. Chem. C*, **2013**, *117*, 21724.
DOI: [10.1021/jp408400c](https://doi.org/10.1021/jp408400c)
 16. Khoa, N. T.; Kim, S. W.; Thuan, D. V.; Tien, H. N.; Hur, S. H.; Kim, E. J.; Hahn, S. H.; *RSC Adv.*, **2015**, *5*, 63964.
DOI: [10.1039/C5RA09620K](https://doi.org/10.1039/C5RA09620K)
 17. Jin, Z.; Zhang, Y. X.; Meng, F. L.; Jia, Y.; Luo, T.; Yu, X. Y.; Wang, J.; Liu, J. H.; Huang, X. J.; *J. Hazard. Mater.*, **2014**, *276*, 400.
DOI: [10.1016/j.jhazmat.2014.05.059](https://doi.org/10.1016/j.jhazmat.2014.05.059)
 18. Men, X.; Chen, H.; Chang, K.; Fang, X.; Wu, C.; Qin, W.; Yin, S.; *Appl. Catal. B: Environ.*, **2016**, *187*, 367.
DOI: [10.1016/j.apcatb.2016.01.052](https://doi.org/10.1016/j.apcatb.2016.01.052)
 19. Liu, X.; Pan, L., Lv, T.; Lu, T.; Zhu, G.; Sun, Z.; Sun, C.; *Catal. Sci. Technol.*, **2011**, *1*, 1189.
DOI: [10.1039/C1CY00109D](https://doi.org/10.1039/C1CY00109D)
 20. Liu, X.; Pan, L.; Zhao, Q.; Lv, T.; Zhu, G.; Chen, T.; Lu, T.; Sun, Z.; Sun, C.; *Chem. Eng. J.*, **2012**, *183*, 238.
DOI: [10.1016/j.cej.2011.12.068](https://doi.org/10.1016/j.cej.2011.12.068)
 21. Wang, C.; Cao, M.; Wang, P.; Ao, Y.; Hou, J.; Qian, J.; *Appl. Catal. A: Gen.*, **2014**, *473*, 83.
DOI: [10.1016/j.apcata.2013.12.028](https://doi.org/10.1016/j.apcata.2013.12.028)
 22. Parlak, O.; Tiwari, A.; Turner, APF.; Biosensing and Nanomedicine-VIII at SPIE Optics and Photonics, **2015**.
 23. Zhao, X.; Hu, B.; Ye, J.; Jia, Q.; *J. Chem. Eng. Data*, **2013**, *58*, 2395.
DOI: [10.1021/jc400384z](https://doi.org/10.1021/jc400384z)
 24. Yang, Y.; Ren, L.; Zhang, C.; Huang, S.; Liu, T.; *ACS Appl. Mater. Interf.*, **2011**, *3*, 2779.
DOI: [10.1021/am200561k](https://doi.org/10.1021/am200561k)
 25. Akhavan, O.; *Carbon*, **2011**, *49*, 11.
DOI: [10.1016/j.carbon.2010.08.030](https://doi.org/10.1016/j.carbon.2010.08.030)
 26. Ahmad, M.; Ahmed, E.; Hong, Z. L.; Xu, J. F.; Khalid, N. R.; Elhissi, A.; Ahmed, W.; *Appl. Surf. Sci.*, **2013**, *274*, 273.
DOI: [10.1016/j.apsusc.2013.03.035](https://doi.org/10.1016/j.apsusc.2013.03.035)
 27. Sandesh, Y.; Sawant; Cho, M.H.; *RSC Adv.*, **2015**, *5*, 97788.
DOI: [10.1039/C5RA22372E](https://doi.org/10.1039/C5RA22372E)
 28. Ravi Kant U.; Navneet S.; Susanta Sinha R.; *RSC Adv.*, **2014**, *4*, 3823.
DOI: [10.1039/C3RA45013A](https://doi.org/10.1039/C3RA45013A)
 29. Larson, K.; Clark, A.; Appel, A.; Dai, Q.; He, H.; Zygmunt S.; *RSC Adv.*, **2015**, *5*, 65719.
DOI: [10.1039/C5RA13048D](https://doi.org/10.1039/C5RA13048D)
 30. Hatem, M.; Emilien, G., Kevin, M.t, Halima, A.; Ghouti, M.; Raphaël, S.; *Appl. Catal. B: Environ.*, **2016**, *185*, 11.
DOI: [10.1016/j.apcatb.2015.12.007](https://doi.org/10.1016/j.apcatb.2015.12.007)
 31. Susanta, B.; Moumita, P.; Atanu, N.; Sunirmal J.; *J. Alloys and Comp.*, **2016**, *669*, 177.
DOI: [10.1016/j.jallcom.2016.02.007](https://doi.org/10.1016/j.jallcom.2016.02.007)
 32. Zhang, X. F.; Xi, Q.; *Carbon*, **2011**, *49*, 3842.
DOI: [10.1016/j.carbon.2011.05.019](https://doi.org/10.1016/j.carbon.2011.05.019)
 33. Rao, C. N. R.; Rakesh, V.; *Materialstoday*, **2010**, *13*, 34.
DOI: [10.1016/S1369-7021\(10\)70163-2](https://doi.org/10.1016/S1369-7021(10)70163-2)
 34. Anastasios, S.; Georgia, P.; Nikos, T.; *Beilstein J. Nanotechnol.*, **2014**, *5*, 1580.
DOI: [10.3762/bjnano.5.170](https://doi.org/10.3762/bjnano.5.170)
 35. Francesco, B.; Nikolaos, B.; Minas, M. S.; Marika, S.; Carlo, A.; Mauro, G.; Vittorio, P.; Emmanuel, S.; Emmanuel, K.; *Adv. Funct. Mater.*, **2015**, *25*, 3870.
DOI: [10.1002/adfm.201501052](https://doi.org/10.1002/adfm.201501052)
 36. Moussa, H.; Giro, E.; Mozet, K.; Alem, H.; Medjahdi, G.; Schneider, R.; *Appl. Catal. B: Environ.*, **2016**, *185*, 11.
DOI: [10.1016/j.apcatb.2015.12.007](https://doi.org/10.1016/j.apcatb.2015.12.007)
 37. Kavitha, M. K.; Suresh, C. P.; Pramod Gopinath; John, H.; *J. Environ. Chem. Eng.*, **2015**, *3*, 1194.
DOI: [10.1016/j.jece.2015.04.013](https://doi.org/10.1016/j.jece.2015.04.013)
 38. Phong, D. T.; Sudip, K. B.; Stevin, S. P.; James, B.; Wong, L. H.; Loo, S. C. J.; *Nanoscale*, **2012**, *4*, 3875.
DOI: [10.1039/C2NR30881A](https://doi.org/10.1039/C2NR30881A)
 39. Chun, H. H.; Lee, J. Y.; Lee, J. H.; Jo, W. K.; *Ind. Eng. Chem. Res.*, **2016**, *55*, 45.
DOI: [10.1021/acs.iecr.5b02751](https://doi.org/10.1021/acs.iecr.5b02751)
 40. Prathik, R.; Arun Prakash, P.; Liang, C. T.; Chang, H. T.; *Environ. Sci. Technol.*, **2013**, *47*, 6688.
DOI: [10.1021/es400422k](https://doi.org/10.1021/es400422k)
 41. Khalid, N. R. E.; Ahmed, E.; Hong, Z.; Sana, L.; Ahmed, M.; *Current Appl. Phys.*, **2013**, *13*, 659.
DOI: [10.1016/j.cap.2012.11.003](https://doi.org/10.1016/j.cap.2012.11.003)
 42. Zhou, K.; Zhu, Y.; Yang, X.; Jiang, X.; Li, C.; *New J. Chem.*, **2011**, *35*, 353.
DOI: [10.1039/C0NJ00623H](https://doi.org/10.1039/C0NJ00623H)
 43. Shirzad-Siboni, M.; Farrokhi, M.; Cheshmeh Soltani, R. D.; Khataee, A.; Tajassosi, S.; *Ind. Eng. Chem. Res.*, **2014**, *53*, 1079.
DOI: [10.1021/ie4032583](https://doi.org/10.1021/ie4032583)
 44. Wang, C.C.; Du, X.D.; Li, J.; Guo, X. X.; Wang, P.; Zhang, J.; *Appl. Catal. B: Environm.*, **2016**, *193*, 198.
DOI: [10.1016/j.apcatb.2016.04.030](https://doi.org/10.1016/j.apcatb.2016.04.030)
 45. Deepak kumar, P.; Gajendra Kumar, P.; Parida K.M.; Singh S.K. *Chem. Eng. J.*, **2014**, *255*, 78.
DOI: [10.1016/j.cej.2014.06.039](https://doi.org/10.1016/j.cej.2014.06.039)
 46. Ramana, P.V.; Viswadevarayalu, A.; Janardhan Reddy, K.; Varada Reddy, A.; Adinarayana Reddy, S.; *Korea. J. Chem. Eng.*, **2016**, *33*, 456.
DOI: [10.1007/s11814-015-0145-4](https://doi.org/10.1007/s11814-015-0145-4)
 47. Purna, K.B.; Priyakshree B.; Gitashree D.; Chaitanya K.K. Indrapal K.; Manjusha V. S.; Pallabi P.; Dulen S.; Das, M.R.; *RSC Adv.*, **2016**, *6*, 11049.
DOI: [10.1039/C5RA25035H](https://doi.org/10.1039/C5RA25035H)
 48. Wu, W.; Roy, V. L.; *Nanoscale*, **2015**, *7*, 38.
DOI: [10.1039/C4NR04244A](https://doi.org/10.1039/C4NR04244A)
 49. Guohui, Dong, G.; Zhang, L.; *J. Phys. Chem. C*, **2013**, *117*, 4062.
DOI: [10.1021/jp3115226](https://doi.org/10.1021/jp3115226)

